

VIABILITY

Comparison of Late Enhancement Cardiovascular Magnetic Resonance and Thallium SPECT in Patients with Coronary Disease and Left Ventricular Dysfunction

Maria Ansari,^{1,4} Phillip A. Araoz,² Stephen K. Gerard,^{2,4}
Norbert Watzinger,² Gunnar K. Lund,² Barry M. Massie,^{1,3,4}
Charles B. Higgins,^{2,4} and David A. Saloner^{2,4,*}

¹Division of Cardiology, ²Department of Radiology, and ³Department of Medicine and Cardiovascular Research Institute, University of California, San Francisco, California, USA

⁴Radiology Service, San Francisco VA Medical Center, San Francisco, California, USA

ABSTRACT

Purpose: Late enhancement magnetic resonance imaging (MRI) was compared with thallium-201 rest-redistribution single photon emission computed tomography (SPECT) in patients with reduced left ventricular (LV) function and prior myocardial infarction (MI). *Background:* Hyperenhancement on contrast cardiac MRI using gadolinium diethylenetriamine pentaacetic acid (Gd-DTPA) has been reported to identify nonviable myocardium. Comparisons of MRI and thallium-201 SPECT have recently been reported. This study focuses on the comparison of these modalities specifically in patients with ischemic heart failure, where viability determination is most clinically relevant. *Methods:* Fifteen patients with LV dysfunction and prior MI [mean ejection fraction (EF) $35 \pm 11\%$] underwent thallium-201 rest-redistribution scintigraphy and contrast MRI on separate days. Each short axis slice was divided into six 60-degree segments, and correlations between MRI and scintigraphy were made on viability detection for each segment. For SPECT, the mean uptake score was calculated from the average of all percent relative activity values throughout each segment. Areas with $<50\%$ of maximal thallium uptake were considered nonviable. On MRI, regions with increased signal intensity after an injection of 0.1 mmol/kg Gd-DTPA were considered nonviable. *Results:* A total of 558 segments were analyzed. Overall, there was a strong inverse relationship between the area of hyperenhancement

*Correspondence: David A. Saloner, Ph.D., Department of Radiology (114D), 4150 Clement St., San Francisco, CA 94121, USA; Fax: (415) 750-6938; E-mail: saloner@itsa.ucsf.edu.

on MRI and diminished thallium-201 uptake on SPECT ($r = -0.51$, $P < 0.001$). There was a significant correlation between the imaging methods for each individual segment, except for the inferior-septal segment ($r = -0.38$, $P < 0.08$). *Conclusions:* In patients with LV dysfunction and prior MI, our data suggest MRI hyperenhancement significantly correlates with myocardial nonviability by thallium-201 SPECT. Correlations were weaker in the inferior-septal region, which may be due to SPECT attenuation artifact.

Key Words: Heart failure; Magnetic resonance imaging; SPECT; Myocardial infarction.

INTRODUCTION

Identifying the extent of viable myocardium is important when making therapeutic decisions regarding revascularization of patients with chronic angina and left ventricular (LV) dysfunction with previous known myocardial infarction (Allen et al., 1996; Rahimtoola, 1989).

Several investigators have recently reported that late enhancement on contrast cardiac magnetic resonance imaging (MRI) using gadolinium diethylenetriamine pentaacetic acid (Gd-DTPA) injection identifies infarcted myocardium regardless of age or location of infarct (Kim et al., 1999; Ramani et al., 1998; Wu et al., 2001). Gadolinium distributes in the extracellular space and therefore relies on loss of myocardial cellular membrane integrity to demonstrate enhancement in acute infarctions. The presence of contrast enhancement suggests myocardial damage at the cellular level and is consistent with an area of myocardial injury or necrosis. In one recent study, the absence of contrast enhancement on cardiac MRI was found to predict improved myocardial function in response to revascularization, although the study was not limited to patients with reduced LV function (Kim et al., 2000).

Previous studies with single photon emission computed tomography (SPECT) thallium scintigraphy have also shown that it predicts recovery of functional myocardium after revascularization (Iskandrian et al., 1983; Ragosta et al., 1993). The goal of the current study was to use late enhancement MRI to evaluate myocardial infarction and viability specifically in patients with reduced LV function and known coronary artery disease and compare the MRI findings with a standard method of determining viability using thallium-201 rest-redistribution.

METHODS

Study Population

Patients with a prior history of myocardial infarction and left ventricular dysfunction who were being

evaluated with rest-redistribution thallium scintigraphy for the question of viability were recruited prospectively from the Chronic Heart Failure clinic at the San Francisco Veteran's Affairs Medical Center between July 1, 2000 and May 31, 2001. Patients were included in the study if they had the following features: 1) older than 21 years; 2) documented history of myocardial infarction based on electrocardiogram or clinical history of chest pain associated with elevated cardiac markers (troponin-I or CPK-MB); 3) ejection fraction less than 50% by echocardiography or cardiac catheterization; 4) and a question of myocardial viability for which rest-redistribution scintigraphy had been ordered by the patient's provider. Exclusion criteria were: 1) contraindications for MRI such as an implantable cardiac device, ferromagnetic clips or intracranial clips; 2) pregnancy; 3) history of problems with iron metabolism or storage (such as hemochromatosis); 4) history of allergic reaction to gadolinium; 5) a clinically unstable medical condition such as hypotension requiring pressor support, ongoing chest pain, or persistent arrhythmias other than atrial fibrillation; 6) inability to give informed consent; and 7) an intercurrent cardiovascular event between imaging studies such as revascularization or myocardial infarction.

Patients underwent thallium scintigraphy and contrast MRI on separate days. The protocol was approved by the institutional Committee on Human Research, and informed written consent was obtained prior to the study.

Imaging Techniques

Thallium-201 Scintigraphy

Images were obtained on patients in the supine position using a Trionix triple headed gamma camera and were obtained at 15–20 minutes (rest images) and again at 4 hours (redistribution images). Following intravenous injection with 3.5 mCi Thallium-201, ungated SPECT was acquired with low energy high-resolution collimation for 15 minutes using summed



segmented acquisitions (Germano et al., 1994; Nakajima et al., 1998). Raw data was acquired in a 64×32 matrix with 3° steps using continuous acquisition. All 360 degrees of data (i.e., from all three detectors) were used for acquisition using filtered back projection with a Butterworth filter, order of 5 and cutoff of 0.45. Side-by-side rest and redistribution SPECT slices were displayed in conventional formats using the standard three cardiac planes of reconstruction (vertical and horizontal long-axis and short-axis slices). Slice thickness was 1 cm.

MRI

Patients underwent MRI imaging in the supine position. A body-surface coil and electrocardiograph (ECG) leads were placed on the chest. Images were acquired using two posterior elements from the spine array on the table, and the two elements of the body phased-array surface coil. Imaging was performed in a 1.5 Telsa Siemens Magnetom MRI scanner (Siemens, Erlangen, Germany). The true long axis and short axis of the left ventricle were determined from a series of rapid ungated scout images. Cardiac cine images were obtained along the horizontal and vertical long axes views using breath-hold acquisitions with a segmented gradient-recalled echo (GRE) technique. The cardiac cycle was partitioned into cardiac phases of 56 ms duration and nine lines were acquired in each phase. Imaging parameters were: repetition time, TR/echo time, TE/flip angle = 6 ms/4 ms/25. An asymmetrical field of view of $380 \text{ mm} \times 285 \text{ mm}$ with a matrix of 256×99 providing a pixel size of $1.5 \text{ mm} \times 2.9 \text{ mm}$ was used. Images were acquired at 56 ms intervals through the cardiac cycle and typically required a breath-hold of less than 10 seconds. Cine images were then acquired along the short axis from the apex to the base of the left ventricle with 6-mm slices at 1-cm spacing. Patients then received 0.1 mmol/kg Gd-DPTA hand injected over 1 minute through a previously inserted antecubital intravenous catheter followed by a saline flush. After a delay of 10 minutes, we began to acquire the postcontrast images. Inversion recovery segmented GRE images were acquired at end diastole along the short axis with 1-cm-thick slices at the same locations as for the cine images using a breath-hold acquisition mode. The most appropriate inversion delay time was evaluated for each patient before collecting the full set of short-axis images. For a single level through the middle of the ventricle, images were acquired starting with an inversion delay time of 200 ms and lengthening the delay time by 50 ms until the point of maximal suppression of myocardial tissue signal was established. In each case that value was

close to 300 ms and was used in the collection of the full set of short-axis images.

Image Analysis

Alignment of the Images

The thallium-201 scintigraphy images were initially aligned with the MRI images using the insertion of the right ventricular free wall onto the left ventricle as a reference. First, the long-axis images from each modality were used to select the midventricular short-axis image independently. The images were then aligned at the midventricular short-axis level and verification was made of the number of slices from midventricle to the base and to the apex for both the thallium-201 SPECT and the MRI images. The midventricular short-axis slice was divided into six 60° segments using the right ventricular free wall insertion as a reference (Fig. 1). The orientation of the six-segment model, once determined from the midventricular slice, was kept constant for the remaining slices. The slices were then numbered from apex to base, and all future comparisons were done on the corresponding aligned segments between thallium-201 SPECT and MRI. Analysis was done separately from the time of alignment and in random order.

Thallium-201 Scintigraphy

The scintigraphic images were analyzed independently by a nuclear physician who was blinded to the patient and to the MRI results. The rest images were used for analysis if there was no difference between rest and redistribution. If there was evidence of further thallium uptake on redistribution images, then those images were

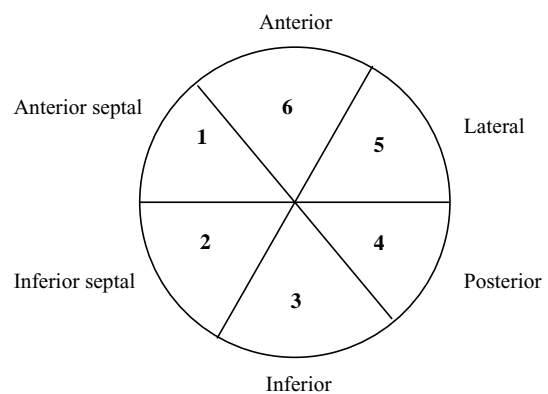


Figure 1. Schematic of the six-segment model of the left ventricle in short-axis view at the midventricular level used for MRI and thallium SPECT studies.

Copyright © Marcel Dekker, Inc. All rights reserved.

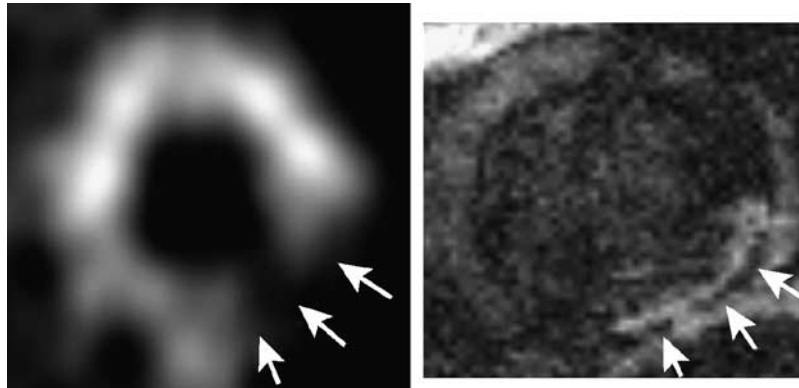


Figure 2. Midventricular short-axis slice of left ventricle showing corresponding slices for thallium-201 SPECT and contrast MRI images with a nonviable inferior–posterior region. The thallium image (left) shows decreased uptake in the inferior–posterior region (arrows), and the MRI (right) shows an area of late enhancement in the same region (arrows).

used for the analysis. For each SPECT study, short-axis slices were analyzed using circumferential profiles. For each subject, the maximum counts per pixel from the entire set of short axis slices was used as the denominator to determine the relative count distribution for all slices analyzed. Each short-axis slice was divided into six 60° segments using the right ventricular free wall insertion as a reference (Fig. 1). For each segment, the mean uptake score was calculated from the average of all percent relative activity values throughout that segment. Areas that were $<50\%$ of maximal uptake were considered nonviable (Ragosta et al., 1993).

MRI

Left ventricular volumes, mass, and ejection fraction were calculated from MRI cine short-axis views using the Argus software package from Siemens Medical Systems. Two observers who were blinded to the patient and to the results of the thallium scintigraphy analyzed the MRI images independently. The images analyzed were obtained at 10 minutes after injection of Gd-DTPA. Analysis of contrast enhancement on the MRI images (Fig. 2) was performed using NIH image, version 1.61 (National Institutes of Health, Bethesda, MD; available at <http://rsb.info.nih.gov/nih-image/>). The short axis images were divided into six equal segments (60° each) beginning with the insertion of the right ventricular free wall on the anterior wall of the left ventricle and moving counterclockwise (Fig. 1). The ventricle was further divided into 1 cm segments from apex to base in the short-axis view. The area of hyperenhancement within each segment was measured and then divided by the total area of that segment. This

was defined as the percentage hyperenhancement of each segment.

Statistical Analysis

All continuous variables are reported as mean \pm standard deviation (SD). The percent of pixels that enhanced on MRI for each segment was then compared to the percent thallium uptake for the corresponding segment by evaluating the correlation coefficient using the Fisher's r to z transformation (Statview version 5.0.1, Berkeley, CA 1992). The percent thallium uptake was also evaluated as a dichotomous outcome ($<50\%$ uptake, nonviable and $\geq 50\%$ uptake, viable) and compared to quintiles of late enhancement on MRI using chi-square analysis. Interobserver variability between the MRI image readers was evaluated using a Bland–Altman plot. $P < 0.05$ was considered statistically significant.

RESULTS

Baseline Characteristics

Fifteen male patients (mean age \pm SD, 60 ± 9 years) completed both the thallium SPECT and MRI protocols on separate days with a mean time difference between studies of 32 days. Cine-MRI measurements showed left ventricular (LV) ejection fraction of $35\% \pm 11\%$ with an LV mass of 258 ± 67 g, an LV end-diastolic volume of 202 ± 66 mL, and an end-systolic volume of 133 ± 57 mL. Infarcts were classified as Q-wave based on electrocardiographic criteria in 10 of the subjects and non-Q-wave in the remaining five. Baseline characteristics including age and location of infarcts are listed in Table 1.



Table 1. Baseline characteristics of 15 study subjects.

	N (%) or Mean \pm SD
Age, y	60 \pm 9
Male gender	100
Q wave infarction by ECG	67
Age of infarction	
Acute (<30 days)	33
Chronic (>6 months)	60
Subacute (<6 months)	<1
Location of infarction by ECG	
Anterior/septal	40
Inferior	<1
Inferior-lateral	20
Posterior	<1
Indeterminate	13
Left ventricular ejection fraction (%)	35+11
Prior PTCA or CABG	27%

Location of the infarct could not be determined electrocardiographically in two of the subjects.

A total of 558 segments were available for analysis of viability. Two segments were omitted from both the nuclear and MRI analysis due to poor image quality. Interobserver agreement for analysis of MRI images was within two standard deviations 94% of the time based on Bland-Altman analysis.

Correlation Between Late Enhancement MRI and Thallium-201 SPECT

Reduced thallium activity on rest and redistribution images was observed in 89 (16%) of the segments on rest and redistribution images. Of the nonviable segments by thallium imaging, 73 segments (89%) also showed late enhancement on MRI. However, of the 469

Table 2. Correlation^a between percent thallium uptake on thallium-201 SPECT and percent late enhancement on MRI.

Segment	r	P
All segments	-0.51	<0.001
Anterior-septum	-0.61	<0.001
Inferior-septum	-0.18	0.08
Inferior	-0.38	<0.001
Posterior	-0.59	<0.001
Lateral	-0.59	<0.001
Anterior	-0.69	<0.001

^aFisher's r to z transformation was used to evaluate statistical significance of the correlation coefficient.

segments that appeared viable on thallium scintigraphy, 33% (156 segments) showed evidence of some nonviability based on late enhancement on MRI.

The correlation between reduced thallium activity and increased MRI signal intensity are shown in Table 2 for all segments combined and individually for each segment. The strongest relationship between thallium and MRI prediction of nonviable myocardium occurred in the anterior ($r = -0.69$, $P < 0.0001$) and anterior-septal ($r = -0.611$, $P = 0.0002$) segments, which corresponded to segments 6 and 1 in our model. This was expressed as a negative correlation indicating that the greater hyperenhancement on MRI was associated with lesser thallium uptake. There was a statistically significant correlation between the two imaging methods for all segments combined ($r = -0.51$, $P < 0.001$) and for each individual segment, except for the inferior-septal segment ($r = -0.38$, $P < 0.08$).

Degree of Late Enhancement Compared to Thallium-201 Uptake

Left ventricular segments that showed any enhancement (or nonviability) by late enhancement MRI are shown in Fig. 3 with the corresponding viability determination by SPECT as determined by percent thallium uptake. Of the patients with segments of myocardium with the highest percentage (>80%) of

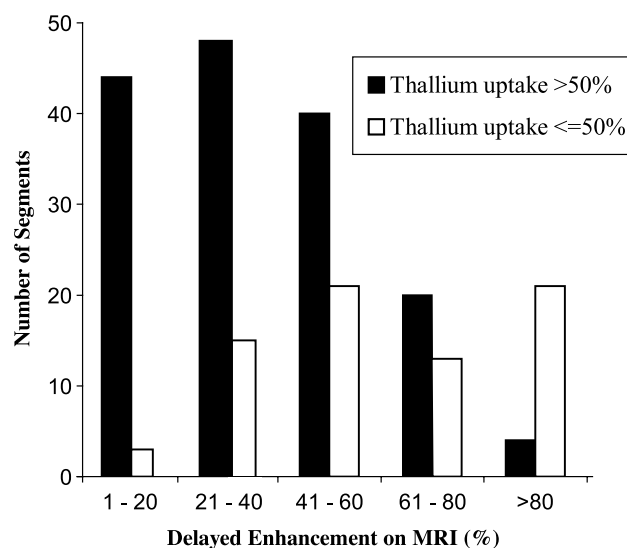


Figure 3. Comparison of viability assessment by thallium SPECT and late hyperenhancement on MRI. Only segments showing hyperenhancement are included. The percent of the area of a segment showing hyperenhancement is the basis for the five groups.

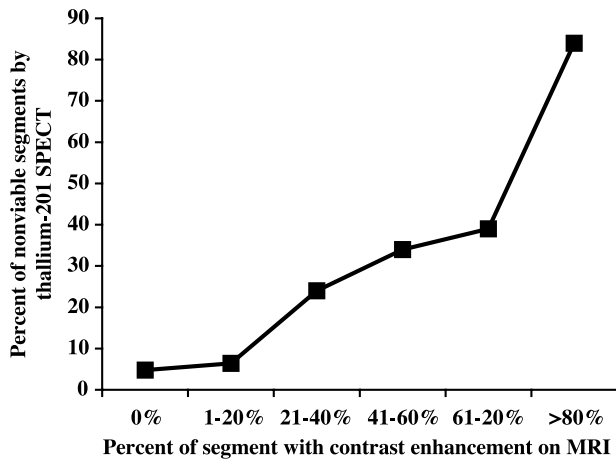


Figure 4. Comparison of thallium-201 SPECT nonviable segments with degree of contrast enhancement by MRI.

hyperenhancement on MRI, indicating nonviable myocardium, 84% (21/25) were also nonviable by thallium SPECT. Conversely, as the percent hyperenhancement diminished on contrast MRI, the percent of segments with thallium SPECT evidence of viability increased (Fig. 4).

DISCUSSION

This study compared results of late enhancement MRI and thallium in patients with significant left ventricular dysfunction and underlying coronary artery disease. This is the clinical group in which viability determination is critical in selecting among therapeutic options. The principal finding was a strong inverse relationship between the degree of late enhancement, the MRI marker of nonviability, and thallium-201 uptake on rest-redistribution scintigraphy.

Comparison Between Thallium-201 Scintigraphy and Late Enhancement MRI

Our data suggest that MRI hyperenhancement significantly correlates with myocardial nonviability by thallium rest-redistribution SPECT imaging at 4 hours. Thallium scintigraphy has been used to determine viability using a rest-redistribution protocol and has had a reported sensitivity to detect viable myocardium up to 90%, but has a lower specificity (Alfieri et al., 1993; Verani, 1992) and in patients with left ventricular dysfunction both sensitivity and specificity decline (Maddahi et al., 1994). It has been criticized for its lack of specificity particularly in the

inferior wall territory, which has been attributed to diaphragmatic attenuation (Zaret et al., 1995). We found in our study that the correlation between late enhancement and thallium scintigraphy determination of viability was strongest in the anterior, anterior-septal, lateral, and posterior regions and weakest in the inferior and inferior-septal regions. We did not perform prone imaging, which may have helped to suppress attenuation artifact and improve specificity in these inferior regions (Esquerre et al., 1989).

We used a cutoff of <50% myocardial thallium uptake to define nonviable tissue (Ragosta et al., 1993). Thallium was compared to Gd-DTPA, which distributes in the extracellular space and may have delayed washout in areas with poor tissue perfusion. Gd-DTPA serves to delineate irreversibly injured myocardium and scar. However, due to the poor spatial resolution of SPECT, one may see a mixture of scar and thallium uptake in infarcted regions suggesting viable myocardium. Therefore, it is possible that in areas of infarcted tissue, we may see both thallium uptake on redistribution images and Gd-DTPA enhancement on MRI. This may in part explain the 33% of segments that appeared nonviable by MRI, but viable by thallium redistribution images.

One advantage of late enhancement cardiac MRI is that it is able to determine the transmural extent of myocardial injury (Kim et al., 2000; Wagner et al., 2003). The higher detection of nonviable myocardium by MRI compared to thallium scintigraphy in our study may also reflect a significant presence of nontransmural infarctions that could be detected by contrast enhancement on MRI but may not demonstrate <50% thallium uptake to meet our criteria for nonviable myocardium. Prior studies comparing MRI and SPECT have shown both improved sensitivity and specificity of MRI over SPECT specifically in acute myocardial infarction patients (Kitagawa et al., 2003) and in areas of non-transmural or subendocardial infarcts (Wagner et al., 2003). In one study by Wagner et al. (2003) involving 91 patients with known or suspected coronary disease, SPECT imaging did not detect subendocardial infarction in 47% of segments felt to be areas of subendocardial scar based on late enhancement MRI. In addition, the investigators used 12 dogs as a gold standard with histochemical staining and found that while late enhancement MRI detected 92% of segments with subendocardial infarct, SPECT only identified 28%.

Hyperenhancement by MRI has been compared with other noninvasive modalities for assessing myocardial viability in patients with coronary disease and LV dysfunction. In one study comparing FDG-PET (18 F-fluorodeoxyglucose positron emission tomography) and contrast enhancement MRI, MRI was able to



detect nonviable myocardium as defined by PET with a sensitivity of 96% and a specificity of 84% in patients with ischemic heart disease and left ventricular dysfunction (Kuhl et al., 2003). In another study comparing PET scanning in patients with ischemic heart failure, 55% percent of segments showing subendocardial hyperenhancement by MRI were classified as normal by PET (Klein et al., 2002). In the PET study, MRI hyperenhancement overestimated the degree of nonviable myocardium detected by PET particularly in areas of nontransmural injury, and this was felt to be secondary to better spatial resolution. This implies that in some instances nontransmural myocardial injury detected by MRI secondary to better spatial resolution may still represent salvageable myocardium based on metabolic function. This is analogous to the presence of thallium-viable segments associated with some degree of MRI enhancement seen in this study. This suggests that the spatial distribution of viable myocardial tissue is such that in small regions where there are adjacent regions of viable tissue and scar tissue, MRI has sufficient resolution to differentiate those two tissue types, whereas partial voluming effects in scintigraphy preclude this differentiation.

Limitations

We used thallium scintigraphy as the “gold standard” for determining viable myocardium. Although this method is a good predictor of functional recovery after revascularization, it is not perfect. For example, the diagnostic accuracy of thallium scintigraphy may be limited by soft-tissue attenuation. There have been recent advances in nonuniform attenuation correction (Hendel et al., 2002), which have yet to be fully validated, and were not available at our center at the time of this study. The use of nitroglycerin to improve myocardial blood flow and therefore viability detection by SPECT has also been reported and our studies were done without nitrates (Sciagra et al., 1997; Tadamura et al., 2003). In addition, we evaluated thallium redistribution at 4 hours instead of 24 hours, however, when thallium is injected at rest; there is no significant increment of further reversibility between 4 and 24 hours (Helber et al., 1999). Finally, we were unable to validate whether the thallium findings predicted improvement with revascularization because only one of our 15 subjects underwent revascularization.

CONCLUSIONS

In patients with ischemic heart disease and known left ventricular dysfunction, late enhancement with Gd-

DTPA correlated with myocardial nonviability as determined by thallium rest-redistribution SPECT images in all segments. The correlation was strongest in the anterior, anterior-septal, lateral, and posterior regions and weakest in the inferior and inferior-septal regions. Contrast enhanced MRI has the potential for being a comprehensive imaging technique for patients with ischemia and left ventricular dysfunction. Regional myocardial function can be assessed by analysis of wall thickening and wall motion on cine breath-hold MRI. In addition, with the use of gadolinium-based contrast agents, viability can be evaluated. The combination of information in one study, both functional wall motion assessment and determination of viability, gives contrast MRI the potential to be a valuable tool for evaluating patients with coronary artery disease and left ventricular dysfunction.

REFERENCES

Alfieri, O., La Canna, G., Giubbini, R., Pardini, A., Zogno, M., Fucci, C. (1993). Recovery of myocardial function. The ultimate target of coronary revascularization. *Eur. J. Cardio-thorac. Surg.* 7:325–330.

Allen, J. W., Cox, T. A., Kloner, R. A. (1996). Myocardial stunning: a post-ischemic syndrome with delayed recovery. *EXS* 76:443–452.

Esquerre, J. P., Coca, F. J., Martinez, S. J., Guiraud, R. F. (1989). Prone decubitus: a solution to inferior wall attenuation in thallium-201 myocardial tomography. *J. Nucl. Med.* 30:398–401.

Germano, G., Kavanagh, P. B., Kiat, H., Van Train, K., Berman, D. S. (1994). Temporal image fractionation: rejection of motion artifacts in myocardial SPECT. *J. Nucl. Med.* 35:1193–1197.

Helber, U., Muller-Schauenburg, W., Hoffmeister, H. M. (1999). Quantification of viable myocardium in multivessel coronary disease: effects of redistribution time after reinjection of thallium-201 and comparison with postrevascularization defect size. *Int. J. Angiol.* 8:36–39.

Hendel, R. C., Corbett, J. R., Cullom, S. J., DePuey, E. G., Garcia, E. V., Bateman, T. M. (2002). The value and practice of attenuation correction for myocardial perfusion SPECT imaging: a joint position statement from the American Society of Nuclear Cardiology and the Society of Nuclear Medicine. *J. Nucl. Med.* 43:273–280.

Iskandrian, A. S., Hakki, A. H., Kane, S. A., Goel, I. P., Mundth, E. D., Segal, B. L. (1983). Rest and redistribution thallium-201 myocardial scintigraphy to predict improvement in left ventricular

Copyright © Marcel Dekker, Inc. All rights reserved.



- function after coronary arterial bypass grafting. *Am. J. Cardiol.* 51:1312–1316.
- Kim, R. J., Fieno, D. S., Parrish, T. B., Harris, K., Chen, E. L., Simonetti, O., Bundy, J., Finn, J. P., Klocke, F. J., Judd, R. M. (1999). Relationship of MRI delayed contrast enhancement to irreversible injury, infarct age, and contractile function. *Circulation* 100:1992–2002.
- Kim, R. J., Wu, E., Rafael, A., Chen, E. L., Parker, M. A., Simonetti, O., Klocke, F. J., Bonow, R. O., Judd, R. M. (2000). The use of contrast-enhanced magnetic resonance imaging to identify reversible myocardial dysfunction. *N. Engl. J. Med.* 343:1445–1453.
- Kitagawa, K., Sakuma, H., Hirano, T., Okamoto, S., Makino, K., Takeda, K. (2003). Acute myocardial infarction: myocardial viability assessment in patients early thereafter comparison of contrast-enhanced MR imaging with resting ²⁰¹Tl SPECT. *Radiology* 226:138–144.
- Klein, C., Nekolla, S. G., Bengel, F. M., Momose, M., Sammer, A., Haas, F., Schnackenburg, B., Delius, W., Mudra, H., Wolfram, D., Schwaiger, M. (2002). Assessment of myocardial viability with contrast-enhanced magnetic resonance imaging: comparison with positron emission tomography. *Circulation* 105:162–167.
- Kuhl, H. P., Beek, A. M., van der Weerd, A. P., Hofman, M. B., Visser, C. A., Lammerstama, A. A., Heussen, N., Visser, F. C., van Rossum, A. C. (2003). Myocardial viability in chronic ischemic heart disease: comparison of contrast-enhanced magnetic resonance imaging with FDG-PET. *JACC* 41:1341–1348.
- Maddahi, J., Schelbert, H., Brunken, R., Di Carli, M. (1994). Role of thallium-201 and PET imaging in evaluation of myocardial viability and management of patients with coronary artery disease and left ventricular dysfunction. *J. Nucl. Med.* 35:707–715.
- Nakajima, K., Taki, J., Michigishi, T., Tonami, N. (1998). Superiority of triple-detector single-photon emission tomography over single- and dual-detector systems in the minimization of motion artefacts. *Eur. J. Nucl. Med.* 25:1545–1551.
- Ragosta, M., Beller, G. A., Watson, D. D., Kaul, S., Gimple, L. W. (1993). Quantitative planar redistribution ²⁰¹Tl imaging in detection of myocardial viability and prediction of improvement in left ventricular function after coronary bypass surgery in patients with severely depressed left ventricular function. *Circulation* 87:1630–1641.
- Rahimtoola, S. H. (1989). The hibernating myocardium. *Am. Heart J.* 117:211–221.
- Ramani, K., Judd, R. M., Holly, T. A., Parrish, T. B., Rigolin, V. H., Parker, M. A., Callahan, C., Fitzgerald, S. W., Bonow, R. O., Klocke, F. J. (1998). Contrast magnetic resonance imaging in the assessment of myocardial viability in patients with stable coronary artery disease and left ventricular dysfunction. *Circulation* 98:2687–2694.
- Sciagra, R., Bisi, G., Santoro, G. M., Zeraushek, F., Sestini, S., Pedenovi, P., Pappagallo, R., Fazzini, P. F. (1997). Comparison of baseline-nitrate technetium-99m sestamibi with rest-redistribution tomography in detecting viable hibernating myocardium and predicting postrevascularization recovery. *JACC* 30:384–391.
- Tadamura, E., Mamede, M., Kubo, S., Toyoda, H., Yamamuro, M., Iida, H., Tamaki, N., Nishimura, K., Komeda, M., Konishi, J. (2003). The effect of nitroglycerin on myocardial blood flow in various segments characterized by rest-redistribution thallium SPECT. *J. Nucl. Med.* 44:745–751.
- Verani, M. S. (1992). Thallium-201 single-photon emission computed tomography (SPECT) in the assessment of coronary artery disease. *Am. J. Cardiol.* 70:3E–9E.
- Wagner, A., Mahrholdt, H., Holly, T. A., Elliott, M. D., Regenfus, M., Parker, M., Klocke, F. J., Bonow, R. O., Kim, R. J., Judd, R. M. (2003). Contrast-enhanced MRI and routine single photon emission computed tomography (SPECT) perfusion imaging for detection of subendocardial myocardial infarcts: an imaging study. *Lancet* 361:374–379.
- Wu, E., Judd, R. M., Vargas, J. D., Klocke, F. J., Bonow, R. O., Kim, R. J. (2001). Visualisation of presence, location, and transmural extent of healed Q-wave and non-Q-wave myocardial infarction. *Lancet* 357:21–28.
- Zaret, B. L., Rigo, P., Wackers, F. J., Hendel, R. C., Braat, S. H., Iskandrian, A. S., Sridhara, B. S., Jain, D., Itti, R., Serafini, A. N., et al (1995). Myocardial perfusion imaging with ^{99m}Tc tetrofosmin. Comparison to ²⁰¹Tl imaging and coronary angiography in a phase III multicenter trial. Tetrofosmin International Trial Study Group. *Circulation* 91:313–319.

Received May 8, 2003

Accepted October 3, 2003



Request Permission or Order Reprints Instantly!

Interested in copying and sharing this article? In most cases, U.S. Copyright Law requires that you get permission from the article's rightsholder before using copyrighted content.

All information and materials found in this article, including but not limited to text, trademarks, patents, logos, graphics and images (the "Materials"), are the copyrighted works and other forms of intellectual property of Marcel Dekker, Inc., or its licensors. All rights not expressly granted are reserved.

Get permission to lawfully reproduce and distribute the Materials or order reprints quickly and painlessly. Simply click on the "Request Permission/Order Reprints" link below and follow the instructions. Visit the [U.S. Copyright Office](#) for information on Fair Use limitations of U.S. copyright law. Please refer to The Association of American Publishers' (AAP) website for guidelines on [Fair Use in the Classroom](#).

The Materials are for your personal use only and cannot be reformatted, reposted, resold or distributed by electronic means or otherwise without permission from Marcel Dekker, Inc. Marcel Dekker, Inc. grants you the limited right to display the Materials only on your personal computer or personal wireless device, and to copy and download single copies of such Materials provided that any copyright, trademark or other notice appearing on such Materials is also retained by, displayed, copied or downloaded as part of the Materials and is not removed or obscured, and provided you do not edit, modify, alter or enhance the Materials. Please refer to our [Website User Agreement](#) for more details.

[Request Permission/Order Reprints](#)

Reprints of this article can also be ordered at

<http://www.dekker.com/servlet/product/DOI/101081JCMR120030582>